

An overview of the $\theta - S$ correlations in Fram Strait based on the MIZEX 84 data

OCEANOLOGIA, 44 (2), 2002.
pp. 243–272.

© 2002, by Institute of
Oceanology PAS.

KEYWORDS

Water masses
Fram Strait
Arctic Mediterranean

PAWEŁ SCHLICHTHOLZ
Institute of Oceanology,
Polish Academy of Sciences,
Powstańców Warszawy 55, PL-81-712 Sopot, Poland;
e-mail: schlicht@iopan.gda.pl

MARIE-NOËLLE HOUSSAIS
Laboratoire d'Océanographie Dynamique et de Climatologie,
UMR7617 CNRS/IRD/Université Pierre et Marie Curie,
4, place Jussieu, 75005 Paris, France

Manuscript received 18 February 2002, reviewed 9 May 2002, accepted 22 May 2002.

Abstract

The water masses in Fram Strait have been analyzed on the basis of hydrographic casts taken in summer 1984 during the MIZEX 84 experiment. In particular, $\theta - S$ diagrams for 16 areas, each 5° in longitude and 1° in latitude, covering the strait from 77°N to 81°N are used to characterize the water masses and discuss their possible origin. Near the surface, the East Greenland Polar Front clearly separates the lighter, cold and fresh Polar Water (PW) from the heavier, warm and saline Atlantic Water (AW). In the upper ocean, the data show a large spreading of the temperature maximum in the $\theta - S$ space associated with different modes of the AW recirculating southward below the PW. Two geographically distinct salinity minima are found in the intermediate layer below the AW. The denser one, in the Boreas Basin, is a feature typical of the Arctic Intermediate Water (AIW) formed by winter convection to the south of the strait, while the lighter one is sandwiched in the Arctic Ocean outflow between the AW layer and the Upper Polar Deep Water (UPDW) characterized by a downward salinity increase. In the deep layer, two salinity maxima are present. The shallower (and warmer) one, associated with the Canadian Basin Deep Water (CBDW), appears all along the East Greenland Slope. A similar but weaker maximum is also found in the southeastern part of the strait. This maximum is perhaps a remnant of the maximum in the East Greenland Current after it has been recirculated back to the strait around the cyclonic gyres of the Nordic Seas. The deeper one appears typically as a near-bottom salinity jump

characteristic of the Eurasian Basin Deep Water (EBDW). The jump is found in two distinct areas of the strait, to the north-west in the Lena Trough and to the south-east in the rift valley of the Knipovich Ridge. The maximum in the former area should have been advected from the Arctic Ocean below the CBDW, while the maximum in the latter area might have originated from haline convection on the adjacent shelves. Some EBDW is trapped in the Molloy Deep over a denser water with salinity decreasing down to the bottom and temperature in the range of the Greenland Sea Deep Water (GSDW).

1. Introduction

Fram Strait is a broad gap between Greenland and Spitsbergen. The strait separates two areas of the Arctic Mediterranean, the Arctic Ocean to the north and the Greenland–Iceland–Norwegian Sea system (the Nordic Seas) to the south. Ice transport as well as $\theta - S$ characteristics of water masses exchanged through Fram Strait and the associated heat and salt fluxes are recognized as a primary issue for climate studies (e.g. Aagaard et al. 1985). A schematic circulation and water mass structure in the Arctic Mediterranean is shown in Fig. 1.

The geographical location of Fram Strait, between two regions with very distinct climatic regimes, is responsible for the presence of a sharp hydrographic front (the East Greenland Polar Front) in the upper water column. The front, which separates waters of atlantic origin from polar waters, is also associated with the ice edge, the outer limit of the arctic ice margin (Fig. 1a). To the north of the strait where a polar type of climate dominates, the sea ice cover and a very stable stratification mostly prevent surface exchanges between the ocean and the atmosphere, except in very restricted open water areas over the shelves. The formation processes in the Arctic Ocean are partly controlled by the inflow from the adjacent seas through interaction with sea ice or with the dense plumes sinking from the surface along the shelf slope (Fig. 1b). Part of this inflow is due to the warm and saline Atlantic Water (AW) transported in the West Spitsbergen Current (WSC) to the east of Fram Strait. That inflow of AW plus the inflow over the Barents Shelf constitutes the only relatively saline water import to the Arctic Ocean (Aagaard & Carmack 1989). The AW inflow and the ice outflow through the strait are also main components of the advective heat budget of the Arctic Ocean (Aagaard & Greisman 1975). The inflowing AW constitutes a subsurface source of sensible heat, while the outflowing ice represents an export of heat deficit related to the large latent heat of fusion of ice. Both the heat and salt contents of the inflowing AW are crucial for the final temperature and salinity characteristics of the intermediate and deep water masses formed in the Arctic Ocean (Rudels et al. 1994, Jones et al. 1995). To the south of the strait, on the other hand, the formation

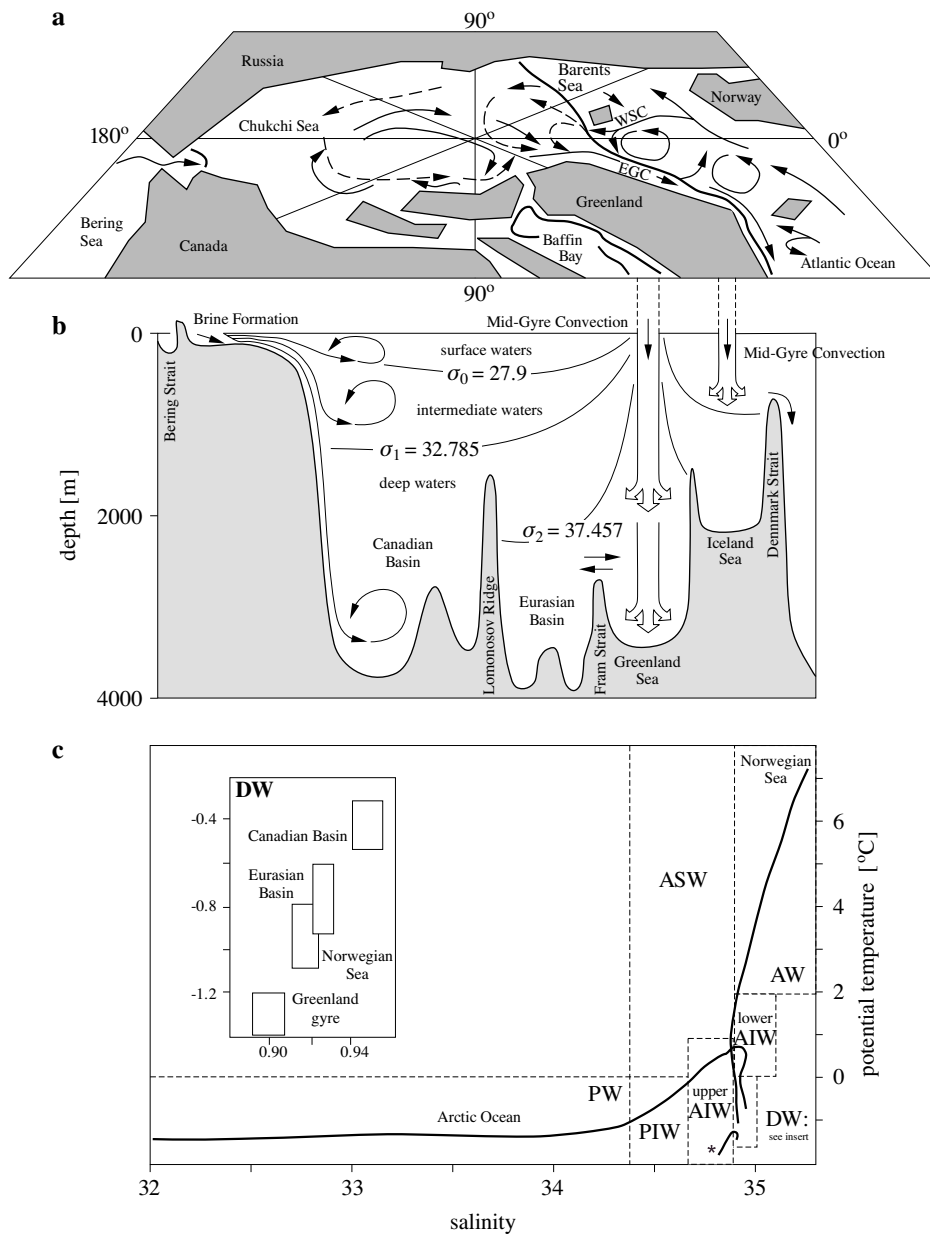


Fig. 1. Schematic circulation and water mass structure in the Arctic Mediterranean (a modified version of Fig. 11 in Aagaard et al. (1985)). The solid (dashed) arrows in (a) correspond to the upper ocean circulation (Atlantic layer circulation in the Arctic Ocean). Acronyms in (a): WSC – West Spitsbergen Current and EGC – East Greenland Current. The solid bold line shows the approximate ice edge position. Acronyms of water masses in (c) are explained in the text. The $\theta - S$ curve marked with an asterisk is for the Greenland gyre

of dense, intermediate or deep water masses is attributed to intense cooling at the ocean surface and to marginally stable stratification, which are both the result of typical subpolar conditions. The efficiency of the water mass formation within the convective gyres is influenced by the sea ice distribution which depends on the local ice formation, but also on the amount of sea ice outflowing from the Arctic Ocean with the East Greenland Current (EGC). The extended ice cover shields the ocean from the atmospheric heat flux and therefore prevents convection. Convection may also be hindered by lateral injections of the fresh, surface Polar Water (PW) from the EGC.

The sill at the depth of 2600 m enables exchanges of deep waters through Fram Strait. The deep circulation and hydrography in the strait are fairly complex owing to the irregular bottom topography (Fig. 2) and to the large variety of deep water masses encountered in the strait (e.g. Friedrich et al. 1995, Rudels et al. 1999). South of the strait, in the Greenland Sea, a cold and relatively fresh deep water mass, the Greenland Sea Deep Water

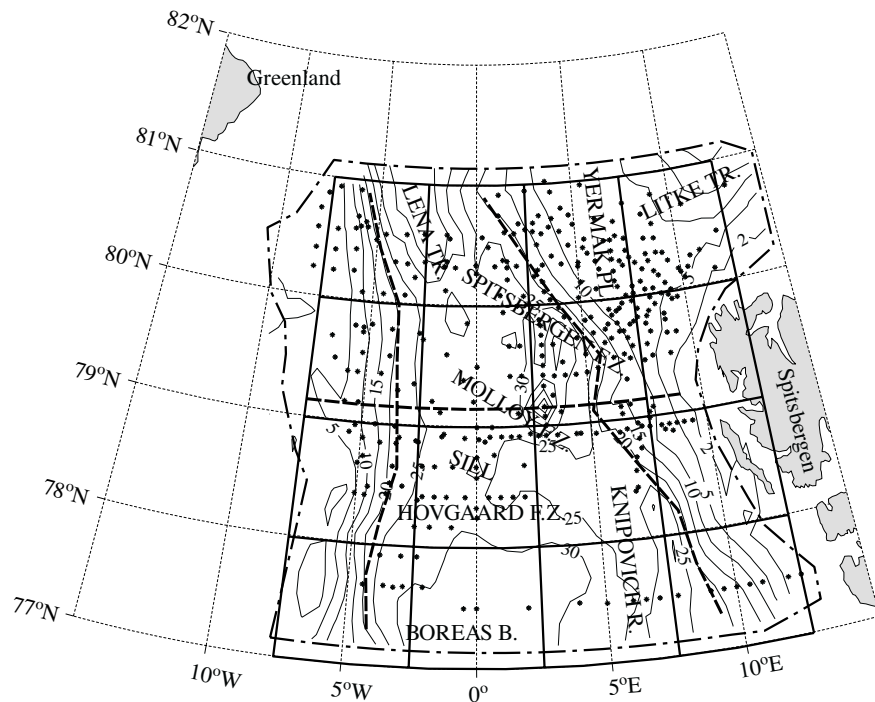


Fig. 2. Bottom topography of Fram Strait (in 10^2 m) and the hydrographic station positions (dots). The dashed-dotted bold line delineates the domain of the inverse model by Schlichtholz & Houssais (1999a), while the dashed bold lines correspond to the position of the hydrographic sections plotted here in Figs. 8–10. The solid bold lines indicate the boxes from which the stations have been used to create the $\theta - S$ diagrams plotted in Figs. 6 and 7

(GSDW), is formed in winter as a result of intense surface cooling (Fig. 1c). North of the strait, in the Eurasian Basin, a warmer and more saline deep water mass, the Eurasian Basin Deep Water (EBDW), is formed essentially through haline convection on the arctic shelves (Aagaard et al. 1985). In addition to these two areas directly connected to Fram Strait, the Arctic Mediterranean includes several other places where deep water mass formation occurs. To the north of the strait, the Canadian Basin Deep Water (CBDW) and the Upper Polar Deep Water (UPDW) are both formed by

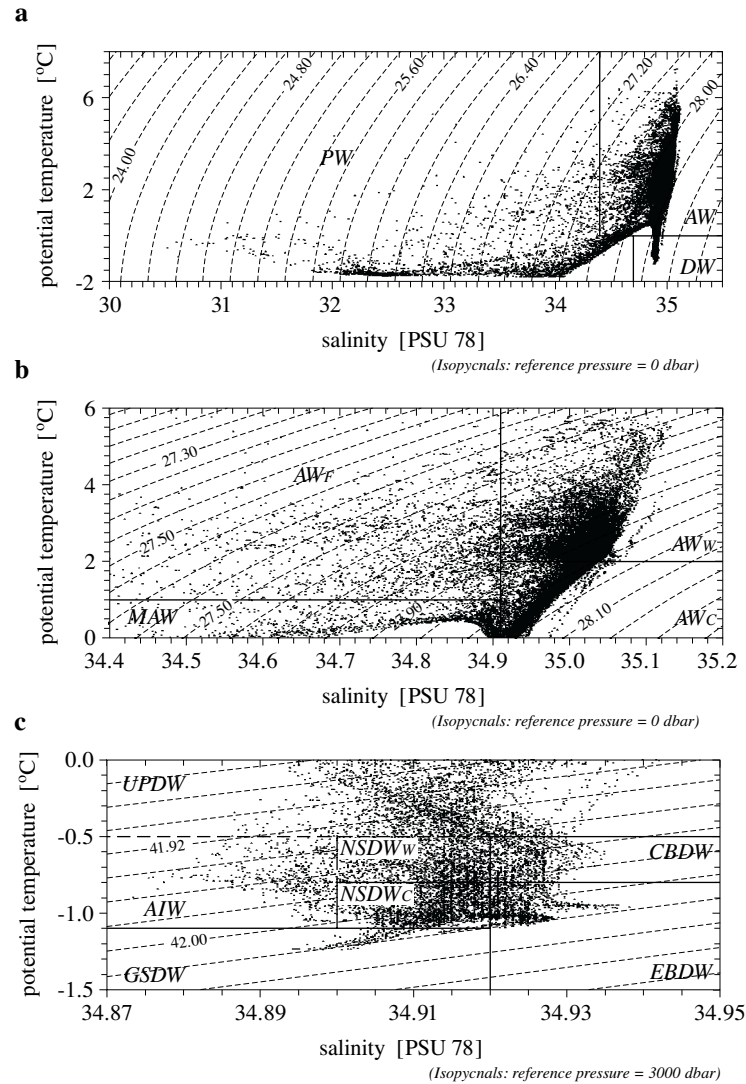


Fig. 3. $\theta - S$ diagram constructed from the MIZEX 84 data for the entire $\theta - S$ range (a), the Atlantic Water range (b) and the Deep Water range (c)

interaction of sinking plumes due to ice formation on the shelves with the inflowing AW (Rudels & Quadfasel 1991). To the south of the strait, the deep saline outflow from the Arctic Ocean mixes with the GSDW along the eastern continental slope of Greenland to form part of the Norwegian Sea Deep Water (NSDW) (Aagaard et al. 1985). Finally, in addition to being a pathway for the above deep water masses, Fram Strait is also recognized as a site of deep water formation: a significant part of the NSDW is thought to be locally produced in the strait (e.g. Aagaard et al. 1991).

In a series of papers (Schlichtholz & Houssais 1999a, b, c) we have presented a comprehensive analysis of the circulation, transports and dynamics in Fram Strait based on analytical and inverse modeling applied to the hydrographic data from the MIZEX 84 experiment (Fig. 2). In particular, the water mass distribution, circulation and associated volume, heat and fresh water fluxes have been studied in Schlichtholz & Houssais (1999b). However, the analysis has been based on interpolated data and essentially involved some integrated quantities such as the layer thickness and mean depth distributions for a given water mass. The classical $\theta - S$ (potential temperature – salinity) analysis has not been carried out. Only an overall $\theta - S$ diagram (Fig. 3) has been used to define the water masses. In section 3, the present study provides a complementary analysis of spatial distributions of the $\theta - S$ correlations in Fram Strait based on the same MIZEX 84 data. Before, in section 2, the schematic pattern of circulation in Fram Strait is briefly described in order to facilitate the analysis. The pattern is based on the results from the inverse model (Schlichtholz & Houssais 1999a), and is therefore consistent with the presented data. The study ends with a discussion in section 4.

2. Circulation pattern

The schematic circulation pattern for the upper and intermediate layers down to a depth of about 800 m in Fram Strait is presented in Fig. 4. The circulation is topographically controlled, with flow mainly occurring along the slopes and shelves, and with recirculations forced by the fracture zones and ridges. The circulation is characterized by a generally southward EGC system on the western side, the EGC proper being defined as the flow along the Greenland Slope and Shelf only, and a generally northward WSC system on the eastern side, the WSC proper covering only the southern portion of the system up to the Yermak Plateau. As it enters the Arctic Ocean, the WSC system interacts with the Litke Trough Current (LiTC), a southwestward current turning northward against the eastern flank of the Yermak Plateau, while at about the same latitude to the west of Fram Strait, the EGC system receives contributions from the Westwind Trough Current (WTC), a southeastward flow over the northern Greenland Shelf.

The dividing line between the EGC and the WSC systems approximately follows the Greenwich meridian. The WSC system exchanges water with the EGC system through counterclockwise recirculations occurring mainly in the Boreas Basin Gyre (BBG), in the Return Atlantic Current (RAC) and in the Spitsbergen Fracture Zone Current (SFZC), the latter two located to the south and north of the Molloy Deep area, respectively. Part of the SFZC participates in a closed cyclonic circulation. In the upper layer, the eastern portion of the WSC splits into four branches. The westernmost branch recirculates in the SFZC. The next branch, the Yermak Slope Current (YSC), is a bottom intensified flow along the western slope of the Yermak Plateau which may partly recirculate farther north in the southward Polar Current (PC). The third branch contributes to the Yermak Plateau Current (YPC) and participates in a cyclonic circulation over the plateau. The easternmost branch, the North Spitsbergen Current (NSC), turns northeastward to follow the shallowest isobaths at the northern tip of Spitsbergen.

Interaction between the EGC and the WSC systems also takes place via the PC which enters the strait from the north over the lower slope to the west of the Yermak Plateau and over the Lena Trough. In the upper layer, the PC splits into a branch feeding the EGC system via the Polar Front Current (PFC) and another branch contributing to the WSC system as a northward recirculation over the Yermak Plateau (the YPC). In the intermediate layer, the PC proceeds farther southward, then recirculates with the SFZC or with the RAC while contributing to an anticyclonic circulation to the east of the Molloy Fracture Zone. In the deep layer (not shown), the PC directly feeds the EGC system via the PFC but the PC may partly originate in a deep recirculation of the EGC itself in the Lena Trough. Deep recirculations also contribute to the EGC system, in particular from the western portion of the WSC which recirculates in the SFZC.

It should be stressed that the above flow pattern is only a quasi-synoptic view based on summer data from a particular year (1984). A simpler pattern arises from a recent analysis of pathways of different water masses in Fram Strait by Rudels et al. (2000). Their inference was based on water mass distribution at a few hydrographic sections from summer 1997. However, major features of the pattern discussed here appear also in the analysis of Rudels et al. (2000). The analysis demonstrates the inflow in the WSC splitting into an inner, outer and recirculating branch corresponding to our NSC, YSC and RAC, respectively, as well as the EGC and an outflow from the Arctic Ocean corresponding to our PC. Details of the pattern in Fig. 4 and the corresponding pattern for the deep flow shown in Schlichtholz

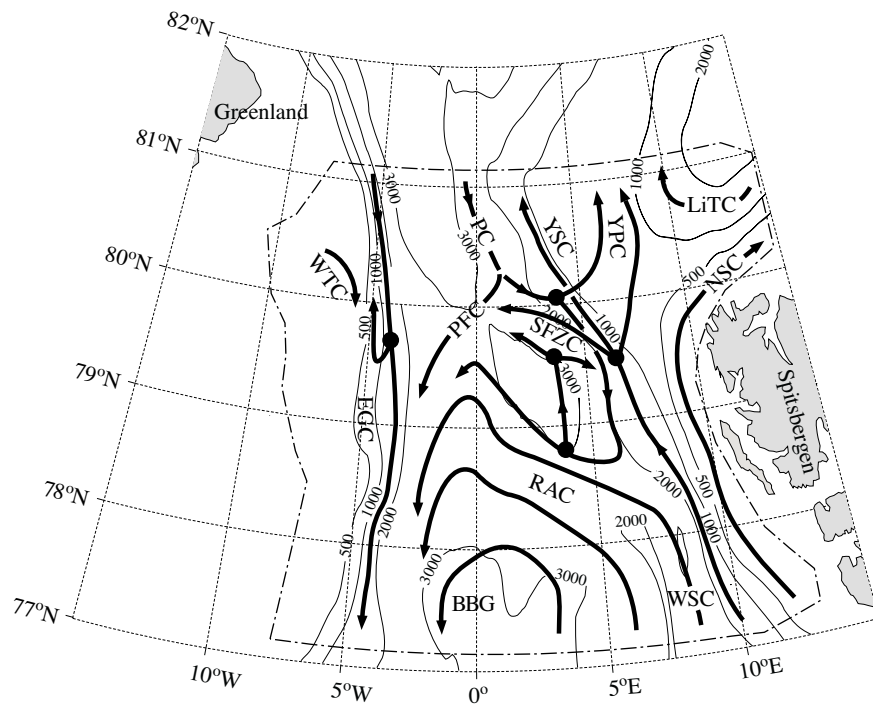


Fig. 4. Schematic representation of the upper and intermediate layer circulation in Fram Strait based on an inverse model (the same as Fig. 19a in Schlichtholz & Houssais (1999a)). The arrows indicate the direction of currents while the dots indicate bifurcations. Also shown are the bathymetry and the model domain. The current acronyms are: BBG – Boreas Basin Gyre; EGC – East Greenland Current; LiTC – Litke Trough Current; NSC – North Spitsbergen Current; RAC – Return Atlantic Current; PC – Polar Current; PFC – Polar Front Current; SFZC – Spitsbergen Fracture Zone Current; WSC – West Spitsbergen Current; WTC – Westwind Trough Current; YPC – Yermak Plateau Current; YSC – Yermak Slope Current

& Houssais (1999a) should be considered as likely but not certain even for summer 1984. First of all, although the MIZEX 84 stations form the largest hydrographic data set ever collected in Fram Strait, they are sparse in certain parts of the strait (Fig. 2). In addition, not all stations covered the total water column. Furthermore, mesoscale eddies are abundant in the area and can distort the overall picture. Finally, the pattern is based on inverse solutions which showed some uncertainty. For instance, the standard deviation of the transport in the WSC system obtained from different solutions was relatively large at some latitudes (see Table 7 in Schlichtholz & Houssais (1999a)). This deficiency may be related, at least partly, to the lack of adequate data.

3. Water mass analysis

3.1. Horizontal distributions of potential temperature and salinity

Horizontal distributions of potential temperature and salinity obtained from the MIZEX 84 data are shown in Fig. 5. The selected levels, 20 m, 800 m and 2000 m, are located in the surface, intermediate and deep layers, respectively, and are each representative of a distinct hydrographic regime. In the surface layer the WSC and the EGC, flowing in opposite directions, are responsible for the bimodal distribution of the $\theta - S$ characteristics in the horizontal, with the fresh cold water of polar origin occupying the northern and western parts of the strait and the warm saline water of atlantic origin located to the south and to the east (Figs. 5a–b). The two modes are separated by the East Greenland Polar Front, which is associated with a high concentration of eddies.

As a result of their different formation scenarios, the deep water masses formed north and south of Fram Strait, when advected into the strait, generate contrasting horizontal $\theta - S$ distributions. By comparison with the situation at the surface, however, the gradients are weaker and of reverse direction, with the warmer and more saline water to the north and to the west (Figs. 5e–f). This is consistent with the concept of the deep outflow from the Arctic Ocean occurring on the western side of the strait while the deep inflow from the Nordic Seas is confined to the east.

In the intermediate layer the $\theta - S$ distribution is more complex. A number of warm, saline eddies are identified along the northeastern side of the Molloy and Spitsbergen Fracture Zones (Figs. 5c–d). The eddies participate in recirculating part of the AW across the strait. The SFZC (Fig. 4) is perhaps a smoothed manifestation of the eddies. Mesoscale eddies are indeed recognized as an important mechanism by which AW may be recirculated from the WSC (Gascard et al. 1988). Another noticeable feature in the intermediate layer distributions is the presence of two areas with relatively low salinity, one to the south, in the BBG, and the other one to the north, confined to the Lena Trough. In the former, the low salinity is correlated with very low temperature and is due to the doming of the deep isopleths into the subsurface layer of the gyre. This southern low salinity feature is disconnected from the northern one which, by comparison, is characterized by higher temperatures.

3.2. Water mass definition

As in Schlichtholz & Houssais (1999b), we here use contiguous rectangular boxes in the $\theta - S$ space in order to characterize 12 different water

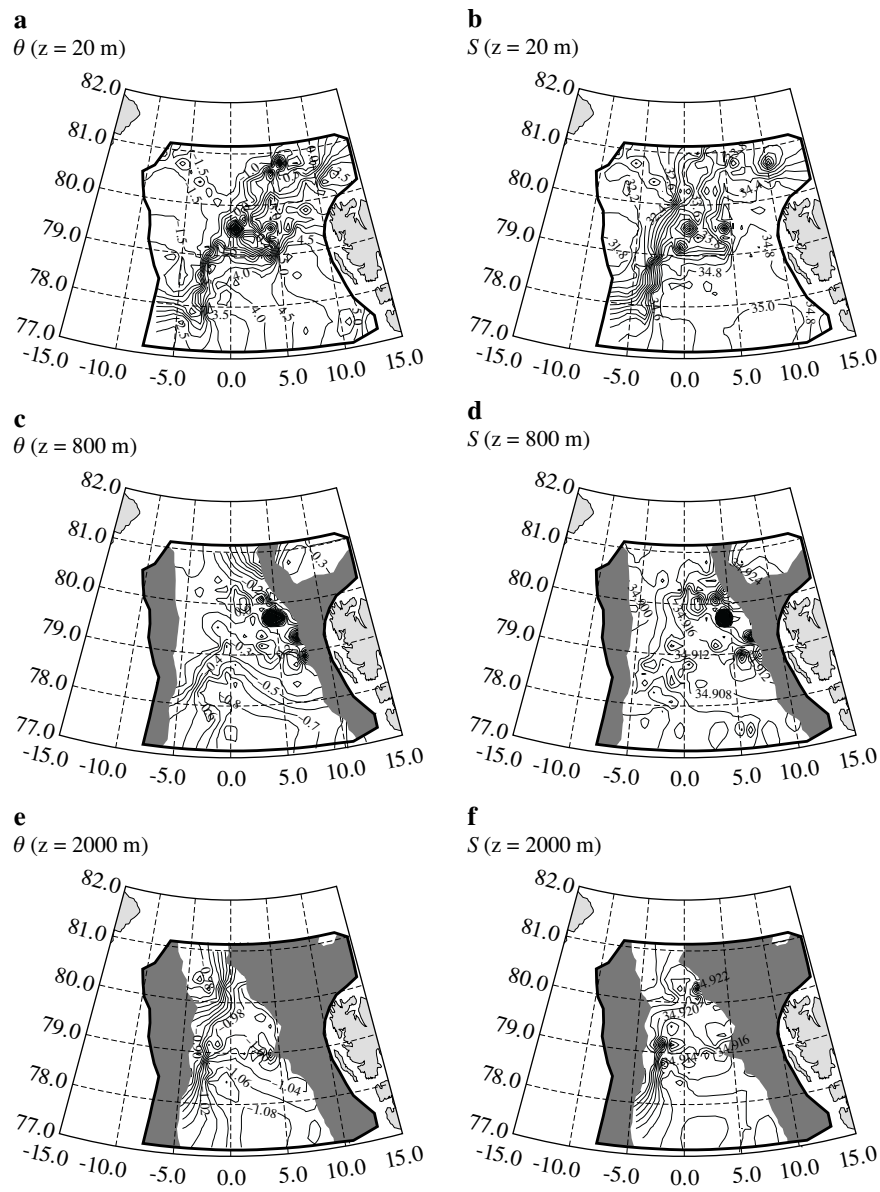


Fig. 5. Horizontal distribution of the potential temperature in $^{\circ}\text{C}$ (left) and salinity (right) from the MIZEX 84 data at 20 m: (a) and (b), 800 m: (c) and (d), 2000 m: (e) and (f). The contour intervals are: 0.5 (a), 0.2 (b), 0.1 (c), 0.004 (d), 0.02 (e) and 0.002 (f) of the corresponding units

masses (Fig. 3). However, some water masses do not fall exactly into these boxes as stressed by the dashed line in Fig. 3c. The departures are explained in Table 1 where the acronyms and $\theta - S$ characteristics of each water mass

Table 1. Water mass characteristics

Acronym ¹	Temperature	Salinity	Depth [m]	σ_0	σ_1	σ_3 ²
PW	$\theta < 0^\circ\text{C}$ $\theta > 0^\circ\text{C}$	$S < 34.7$ $S < 34.4$	65 ± 42	26.81	31.55	40.74
AWw	$\theta > 2^\circ\text{C}$	$S > 34.91$	169 ± 87	27.91	32.55	41.53
AWF	$\theta > 1^\circ\text{C}$	$34.4 < S < 34.91$	71 ± 19	27.77	32.42	41.43
AWc	$0^\circ\text{C} < \theta < 2^\circ\text{C}$	$S > 34.91$	462 ± 115	28.02	32.70	41.77
MAW	$0^\circ\text{C} < \theta < 1^\circ\text{C}$	$34.4 < S < 34.91$	293 ± 117	27.94	32.64	41.74
AIW	$-1.1^\circ\text{C} < \theta < -0.5^\circ\text{C}$ $-0.8^\circ\text{C} < \theta < 0^\circ\text{C}$	$34.7 < S < 34.9$ $34.9 < S < 34.92$ ³	550 ± 200	28.06	32.79	41.95
UPDW	$-0.5^\circ\text{C} < \theta < -0^\circ\text{C}$	$34.7 < S < 34.9$ ⁴	1008 ± 172	28.05	32.77	41.91
NSDWw	$-0.8^\circ\text{C} < \theta < -0.5^\circ\text{C}$ $-0.5^\circ\text{C} < \theta < 0^\circ\text{C}$	$34.9 < S < 34.92$ ⁵ $34.9 < S < 34.92$ ⁶	947 ± 161	28.06	32.79	41.94
CBDW	$-0.8^\circ\text{C} < \theta < -0.5^\circ\text{C}$	$S > 34.92$	1500 ± 138	28.08	32.81	41.97
NSDWc	$-1.1^\circ\text{C} < \theta < -0.8^\circ\text{C}$	$34.9 < S < 34.92$	1610 ± 334	28.08	32.82	42.00
EBDW	$-1.1^\circ\text{C} < \theta < -0.8^\circ\text{C}$	$S > 34.92$	2333 ± 303	28.09	32.83	42.01
GSDW	$\theta < -1.1^\circ\text{C}$	$34.7 < S < 34.92$	2482 ± 300	28.08	32.83	42.02

¹ PW – Polar Water, AWw – warm Atlantic Water, AWF – fresh Atlantic Water, AWc – cold Atlantic Water, MAW – Modified Atlantic Water, AIW – Arctic Intermediate Water, UPDW – Upper Polar Deep Water, NSDWw – warm Norwegian Sea Deep Water, CBDW – Canadian Basin Deep Water, NSDWc – cold Norwegian Sea Deep Water, GSDW – Greenland Sea Deep Water, EBDW – Eurasian Basin Deep Water; ² σ_0 , σ_1 and σ_3 – density in sigma units referred to 0, 1000 and 3000 dbar, respectively, and calculated from the mean temperature and salinity in the considered range; ³ if a salinity minimum is found in the range $-1.1^\circ\text{C} < \theta < -0.5^\circ\text{C}$; $34.7 < S < 34.9$; ⁴ only if the mean $\theta - S$ regression slope is negative; ⁵ if not AIW; ⁶ if not AIW nor UPDW.

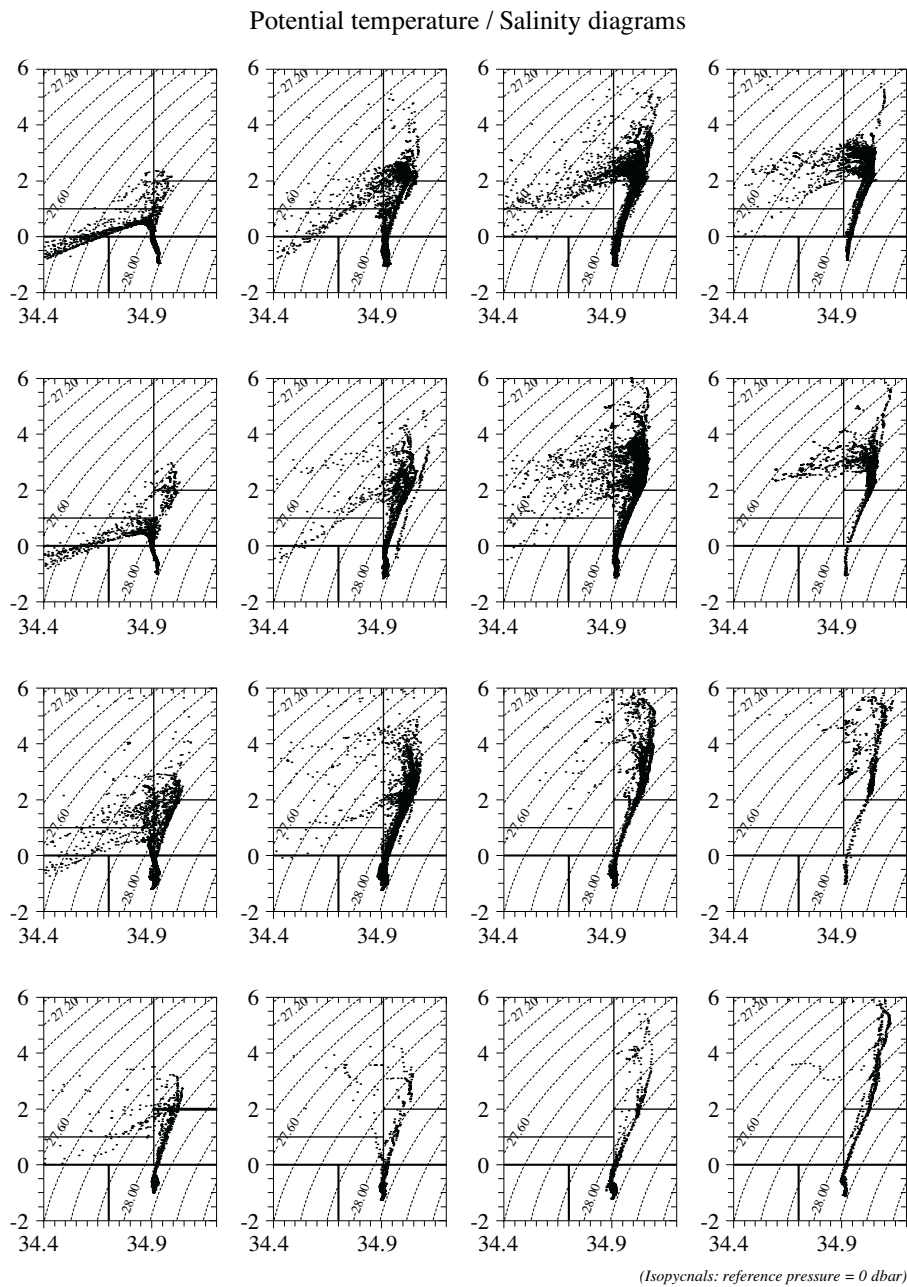


Fig. 6. $\theta - S$ diagrams in the Atlantic Water range constructed from the MIZEX 84 data in the domain extending between 7.5°W and 12.5°E and between 77°N and 81°N for 16 subdomains (see Fig. 2). The upper left diagram corresponds to the northwesternmost subdomain while the lower right diagram corresponds to the southeasternmost subdomain. Salinity is in PSU and temperature is in $^{\circ}\text{C}$

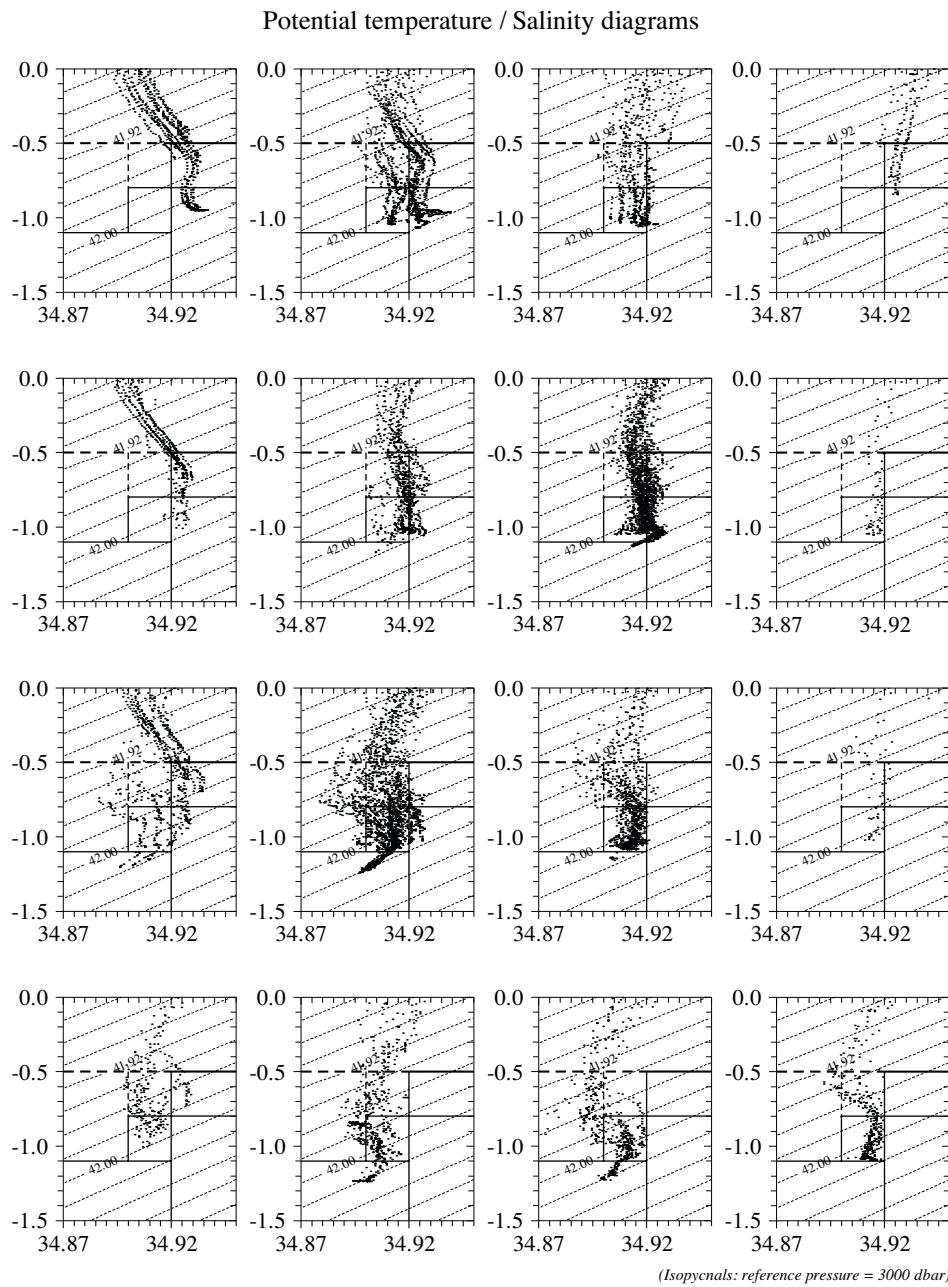


Fig. 7. The same as Fig. 6 except for the Deep Water range

are given together with the mean depth and the potential density referred to the sea surface (σ_0), and the depths of 1000 m and 3000 m (σ_1 and σ_3).

As for the entire Arctic Mediterranean (Fig. 1c), all the water masses

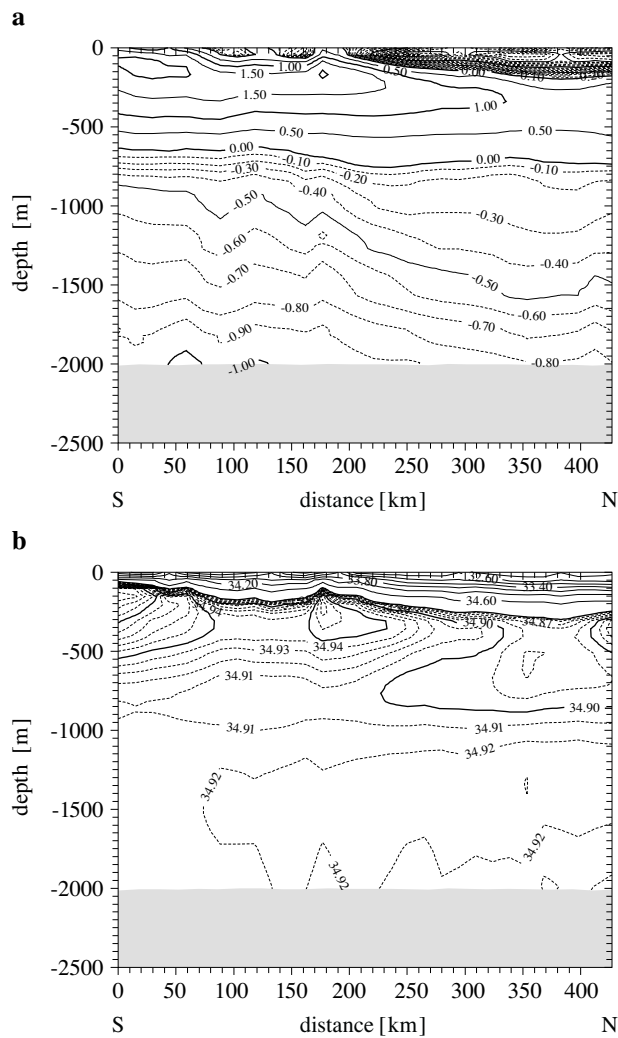


Fig. 8. Vertical distributions of the potential temperature (in $^{\circ}\text{C}$) (a) and salinity (b) along the 2000-m isobath to the west of Fram Strait. The distributions are based on the MIZEX 84 data interpolated using the method described in Schlichtholz & Houssais (1999b). The contour intervals are: 0.1°C in the negative and 0.5°C in the positive temperature range (a); 0.4 for $S < 34.6$, 0.01 for $34.85 < S < 35.1$ and 0.05 for $S > 35.1$ (b)

encountered in Fram Strait (Fig. 3a) derive from two main sources, the AW and the PW. These two source water masses are each representative of a distinct water mass category and are usually separated by the isohaline $S = 34.4$ (Swift & Aagaard 1981) or the isotherm $\theta = 0^{\circ}\text{C}$ (Rudels & Quadfasel 1991). The AW and the PW interact with each other and with

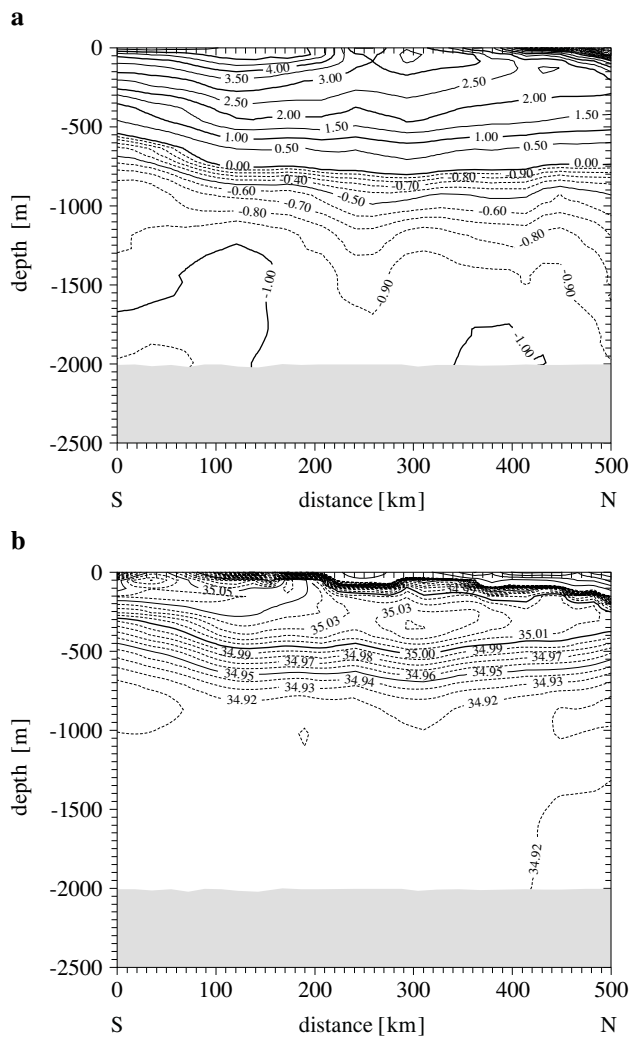


Fig. 9. The same as Fig. 8 except along the 2000-m isobath to the east of Fram Strait

the atmosphere to create a variety of water masses which, in the upper water column, occupy a wide range of $\theta - S$ values and together define the upper water masses but, as the products become denser, enter a third water mass category with more specific characteristics, the Deep Water (DW). The DW is characterized by cold dense products with $\theta < 0^\circ\text{C}$.

Aagaard et al. (1985) considered two types of PW, a surface PW with $S < 34.4$ and a Polar Intermediate Water (PIW) with $S < 34.7$ (Fig. 1c). Here the two types are combined into a single water mass (Fig. 3a).

In the $\theta - S$ space the isohaline $S = 34.7$ separates the light surface PW from the dense DW. In the physical space the two categories are separated by a modified water of atlantic origin, which in the terminology used by Aagaard et al. (1985) is the upper or lower Arctic Intermediate Water (AIW). Their upper AIW includes not only water with positive temperature but also some water with negative temperature originating from the convective gyres of the Nordic Seas (Fig. 1b). This water mass is here considered as a component of the DW category and referred to as the AIW (Fig. 3c). All water with $\theta > 0^\circ\text{C}$ belongs to the AW category (Fig. 3b).

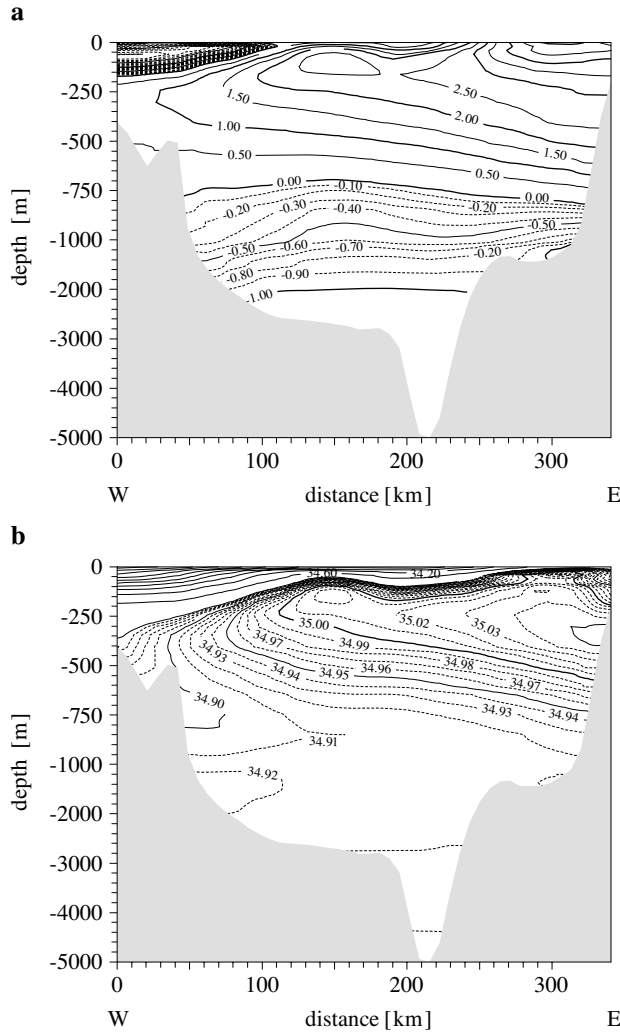


Fig. 10. The same as Fig. 8 except along the parallel 79.15°N

In order to highlight the horizontal contrast of water mass properties, the domain extending between 7.5°W and 12.5°E , and between 77°N and 81°N , has been divided into 16 adjacent subdomains, each covering 5° in longitude and 1° in latitude (Fig. 2). $\theta - S$ diagrams have been prepared in which the data from all stations located within a given subdomain are plotted together, both for the AW range (Fig. 6) and the DW range (Fig. 7). In addition, we also present three vertical sections of potential temperature and salinity constructed from the irregularly spaced data (Fig. 2) according to the procedure outlined in the appendix in Schlichtholz & Houssais (1999b). Two sections follow the 2000-m isobath contour with an approximate north-south orientation, one section along the western slope (Fig. 8) and the other along the eastern slope of the strait (Fig. 9). The third section is zonal, running along 79.15°N (Fig. 10).

3.3. The Polar Water

The PW, possibly the freshest water mass found in Fram Strait (Fig. 3a), is formed by the addition of fresh water products (river run-off, net precipitation) to the inflowing AW in the Arctic Ocean (Rudels 1989). Although the main body of the PW is characterized by negative temperatures, positive temperatures, sometimes larger than 3°C , are not uncommon in summer, for instance, in the Greenland Sea (Swift 1986). We therefore do not restrict the range of possible temperatures covered by the PW. In Fram Strait, the PW moves southward within the EGC system – the EGC proper, WTC, PC and PFC – and partly recirculates northward with the YPC (Fig. 4).

As the lightest water mass, the PW forms a surface layer, which has a wedge-like structure. A frontal zone develops along the southeastern rim of the wedge (Figs. 5a–b) which approximately coincides with the ice edge, in agreement with the abundant eddy activity and the active ice melting reported in the area (Johannessen et al. 1987, Josberger 1987). The PW wedge is stratified, with a strong halocline in the subsurface as a result of the annual course of winter freezing and summer ice melt (Figs. 8–10). The summer surface mixed layer is thin. Observations to the north of Fram Strait indicate that the 100-m thick mixed layer often found in winter (Rudels 1987) retreats in summer to a less than 10-m thick layer maintained by mechanical stirring due to the ice draft (Morison et al. 1987). Instead, underneath the surface, a local close-to-freezing temperature minimum is present (Fig. 3a) at about 50 m, which suggests that summer warming contributes to the restratification process only in the upper part of the halocline (Figs. 8 and 10). As this minimum results in a particular shape of the $\theta - S$ curves, it is often referred to as the ‘knee’ water (e.g. Bourke

et al. 1987). In the lower halocline the PW layer is characterized by positive values of the $\theta - S$ correlation indicative of active heat transfer with the underlying AW (Fig. 6).

3.4. The Atlantic Water and its derived products

The AW is a warm water mass traditionally defined by a lower temperature limit which basically decreases northward as the water loses heat to the atmosphere. In certain areas, such as the Nordic Seas, where it may be necessary to distinguish the AW from fresh arctic products derived from its interaction with sea ice, a correct definition of the AW also requires introducing a lower salinity limit. In the Nordic Seas, the AW is accordingly defined as water with $\theta > 3^\circ\text{C}$ and $S > 34.4$ (Swift & Aagaard 1981). In Fram Strait, we distinguish four modes in the AW range (Fig. 3b), the warm (AWw) and cold (AWc) modes with higher salinity ($S > 34.91$), and the fresh (AWF) and modified (MAW) modes with lower salinity ($34.4 < S < 34.91$). These modes correspond roughly to the modes considered in Rudels & Quadfasel (1991) and Friedrich et al. (1995). The choice of the temperature limit between the AWw and the AWc, $\theta = 2^\circ\text{C}$, is based on a clear difference in the slope of the $\theta - S$ regression line for the two modes (Fig. 6). A lower temperature limit, $\theta = 1^\circ\text{C}$, between the AWF and the MAW better captures the core of the MAW.

3.4.1. Atlantic Water: warm and fresh modes

The warmest and saltiest component of the AW, the AWw, enters Fram Strait from the southeast in the WSC after the Norwegian Atlantic Current has split into two branches at the northern tip of Norway, one branch flowing to the Barents Sea and the other flowing towards the Arctic Ocean through Fram Strait (Fig. 1a). The AWw is therefore more apparent in the eastern part of Fram Strait (Fig. 10), where it appears in the south as well as in the north (Fig. 9). It flows northward within the WSC system: the WSC proper, NSC, YPC, and YSC (Fig. 4). A part recirculates with the RAC and SFZC. Recirculating AWw is indeed found in the EGC as depicted by warm and saline cores at about 150 m in the western part of the strait (Fig. 8). The southernmost core has salinity well above $S = 35.0$.

The AWw outcrops at the surface only in the southeastern part of the domain while, to the north and to the west, it sinks below the PW (Figs. 8–10). If not outcropping at the surface, the AWw is identified as a temperature and salinity maximum which, at the same latitude, weakens westward (Figs. 10 and 6). In the area where the AWw is a surface water mass, the AWw layer is characterized by a fairly uniform salinity profile and a temperature controlled stratification (Fig. 6). At the southeastern tip

of Spitsbergen, its maximum temperature may be as high as 7°C (Fig. 3a). By contrast with winter situations, the atmospheric heat loss and, therefore, the northward temperature gradient in the AWw in the southern part of the domain, appear to be weak in summer (Fig. 6). The temperature gradient, however, persists off the northwestern coast of Spitsbergen where the AWw meets the ice margin. There, the correlated patterns of temperature and salinity are a clear signature of sea ice bottom melting, an important mechanism capable of maintaining a fairly stationary ice edge north of Spitsbergen (Hunkins 1990), and responsible for important modifications of the AW characteristics before the water penetrates into the Arctic Ocean. Indeed, the northward temperature and salinity decrease intensifies in the region of the Yermak Plateau, reaching values of $3 - 4^{\circ}\text{C}$ and 1 PSU per 100 km, respectively (Figs. 5a–b). In this region, admixture of PW and melt water to the AW creates a new mode of AW, the AW_F.

The freshened, but still warm, mode of AW, the AW_F, often referred to, in the Nordic Seas, as the Arctic Surface Water (Swift 1986), is a typical summer surface water formed by interaction of the saline AWw with the fresh PW and with sea ice. It is therefore absent from most of the open water area in Fram Strait, except in the BBG or just against the ice edge where it outcrops at the surface (Figs. 5a–b). The AW_F is one of a few water masses which are (partly) produced in the strait (Schlichtholz & Houssais 1999b). The AW_F essentially spreads underneath the PW as a transition layer between the PW and the AWw (Figs. 9 and 10). As the AW_F sinks underneath the PW, it is less influenced by ice melting and therefore less stratified. Accordingly, the slope of the $\theta - S$ regressions in the AW_F range becomes more isopycnal northwestward (Fig. 6).

3.4.2. Atlantic Water: cold and modified modes

The cold component of the AW, the AW_c, is the densest mode of the AW in Fram Strait (Fig. 3b). It appears nearly everywhere in the strait, except over the shallow shelf areas (Figs. 8–10). The AW_c, wherever it appears, does not outcrop at the surface, at least in summer. It is either capped by some AWw, especially in the WSC system, or, only in the EGC system, forms a maximum temperature and salinity core underneath the PW/AW_F layer (Fig. 6).

In contrast to the AWw, the AW_c is a fairly weakly stratified water mass as shown by a more isopycnal run of the $\theta - S$ curves at temperatures below 2°C than at temperatures above 2°C (Fig. 6). The AW_c in the WSC system is characterized by a gradual downward salinity decrease, probably due to mixing of the AWw with some cold and fresh AIW after winter cooling south of the strait (Aagaard et al. 1985). An important transformation of

some AWw into AWc occurs also in Fram Strait in summer (Schlichtholz & Houssais 1999b). However, some AWw escapes to the Arctic Ocean where a final transition of the AWw into AWc must occur. Some AWw with $\theta > 2^\circ\text{C}$ has been observed, for instance, to the north of the Yermak Plateau (Muench et al. 1992). The Atlantic layer of the Arctic Ocean should also be fed by some of the AWc formed in Fram Strait through intense winter cooling in the WSC (Boyd & D'Asaro 1994). In addition, the input to that layer is due to the advection of water masses transformed in the Barents Sea where similar shapes of the $\theta - S$ curves in the AWw–AWc range to those in Fram Strait have been observed (Swift 1986).

The AWc is a major mode of the AW recirculating southward in Fram Strait. The main core of the RAC, identified as the subsurface saline core with $S > 35.0$ which crosses the 2000-m isobath of the Greenland Slope (Fig. 8) is composed of AWw and also of AWc. Another subsurface saline core ($S > 34.95$) with only a small contribution from the AWw can be attributed either to the northernmost limb of the RAC recirculating to the west of the Molloy Deep or to the recirculation of AWw in the SFZC, north of the Molloy Deep area, associated with a gradual transformation of the AWw into AWc. The presence of the AWc in the northern part of the strait along the slope to the west of the Yermak Plateau and in the Lena Trough (Figs. 6 and 9) is associated with the southward flow of the PC which transfers some AWc from the Arctic Ocean to the PFC and to the RAC (Fig. 4).

Only a little AWc is present in the EGC in the northern part of the strait. Instead, the MAW, the most altered mode of the AW with respect to both temperature and salinity is present there (Fig. 8). The MAW is characterized by a temperature maximum which is a permanent and omnipresent feature in the Arctic Ocean. Depending on the possible paths and transformations in the Arctic Ocean, the temperature maximum acquires different characteristic values (Rudels et al. 1994). The relatively low values of the maximum in the northwestern part of Fram Strait along the Greenland Slope (Fig. 6) suggest that it is indeed advected from the north as a modification of the AW which enters through Fram Strait or across the Barents Sea (Fig. 1a), then flows eastward along the Eurasian continental slope, crosses the Lomonosov Ridge, and finally returns along the Greenland Slope towards Fram Strait (Anderson et al. 1994). In the strait, the MAW has a very limited extent and is almost exclusively found over the Greenland Shelf and Slope. The colder MAW is always found west of the warmer AWc and AWw (Fig. 10). A mixture of these three water masses is present nearly everywhere in the EGC system, leading to a large spreading of the temperature maximum in the $\theta - S$ space (Fig. 6).

3.5. The Deep Water

3.5.1. The lighter modes: Arctic Intermediate Water and Upper Polar Deep Water

The DW range (Fig. 3c) includes not only deep but also intermediate water masses which constitute the lighter mode in the DW range. These intermediate waters occupy roughly the warm or fresh poles of the DW class in the $\theta - S$ space, but owing to their formation processes, they are not consistently defined by prescribed $\theta - S$ ranges. The fresh AIW is defined by a salinity minimum ($S < 34.90$) located in the temperature range $-1.1^\circ\text{C} < \theta < -0.5^\circ\text{C}$. In addition to water at this minimum salinity, the AIW also includes water located above this minimum and characterized by a positive regression slope (increasing salinity for increasing temperature). The salinity minimum in the core of AIW is due to the relatively low salinity of the surface waters of the Greenland Sea gyres which, after winter cooling and sinking to intermediate depths, constitute the main source of AIW. The fresher portion ($S < 34.90$) of the AIW corresponds to the upper AIW as defined by Swift & Aagaard (1981). The pure AIW appears to be restricted to its formation region, the Boreas Basin, since a salinity minimum below 34.90 is present only in the southern part of the strait (Fig. 7). However, a weaker salinity minimum (above 34.90) at $\theta \approx 0.5^\circ\text{C}$ is found all along the continental slope on the eastern side of the Strait (Figs. 7 and 9). Therefore, the AIW appears to be not only trapped within the BBG but also advected northward by the WSC system, while gradually changing its properties as a result of interaction with other water masses. In Schlichtholz & Houssais (1999b), this modified AIW has been included into a warm mode of the NSDW (see also section 3.5.3 below). The slope of the $\theta - S$ regression line above the salinity minimum associated with the pure (or modified) AIW is consistent with the slope in the $\theta - S$ range of the AWc, a water mass which caps the AIW (Fig. 6).

In Fram Strait, the AIW meets the UPDW, which is generally lighter but deeper than the AIW (Table 1). The UPDW is characterized by a negative slope of the $\theta - S$ regression line in the temperature range $-0.5^\circ\text{C} < \theta < 0^\circ\text{C}$ (Rudels et al. 1994). Its salinity is generally higher than 34.88 and increases downward until it reaches the CBDW layer characterized by a salinity maximum at about $\theta = -0.6^\circ\text{C}$. The UPDW is identified as an outflow from the Arctic Ocean guided by the topography, all along the Greenland Slope and in the Lena Trough (Figs. 7 and 8). The lighter part of the UPDW is characterized by a salinity minimum below the AW layer, at $\theta = -0.1^\circ\text{C}$ (Fig. 7). This minimum corresponds to the minimum in the salinity distribution at 800 m (Fig. 5d). A similar minimum is found in

the Eurasian Basin where it is likely to be formed by the inflow of colder and less saline AW from the Barents Sea (Rudels et al. 1994, Schauer et al. 1997). In Fram Strait, the minimum forms a wedge whose thickness decreases eastward (Fig. 10) and southward (Fig. 8). According to Rudels et al. (1999) the minimum in Fram Strait could be a local feature related to the recirculation of the WSC.

3.5.2. Arctic Ocean deep waters: Canadian Basin Deep Water and Eurasian Basin Deep Water

In the deep water range, two salinity maxima ($S > 34.92$) are identified (Figs. 3c and 7). The warmer maximum, between $\theta = -0.8^\circ\text{C}$ and $\theta = -0.5^\circ\text{C}$, represents the CBDW which crosses the Lomonosov Ridge (e.g. Anderson et al. 1994). The strength of the associated salinity maximum suggests that the CBDW is advected to the strait directly from the Canadian Basin without any substantial recirculation in the Eurasian Basin, as suggested first by Anderson et al. (1989). The other deep salinity maximum is colder ($\theta < -0.8^\circ\text{C}$) and represents the EBDW. Only in a limited area of Fram Strait, in the vicinity of the Molloy Deep, does the EBDW overlie the fresher NSDW, therefore appearing as a relative salinity maximum on the $\theta - S$ curve. At several stations, which are mostly located in the Lena Trough where the salinity maximum exceeds 34.935, the water mass is identified as a quasi-isothermic, near-bottom salinity jump (Fig. 7). The near-bottom, cold and saline layer is a typical feature of waters which have experienced the threshold of the freezing point at some time and have then sunk as boundary plumes down the continental slope. The most saline plumes reach deeper levels and stratify the bottom layer. The constant temperature can be explained by the fact that the plumes have the same initial temperature and entrain the same amount of intermediate water (Rudels et al. 1999). A near-bottom salinity jump, having a lower temperature than the jump in the Lena Trough, is also found in the rift valley of the Knipovich Ridge. In this area, the salinity jump may be attributed to nearby haline convection events like those reported by Quadfasel et al. (1988) or Schauer (1995) in Storfjord.

Like the shallower UPDW, the deeper CBDW is advected by the EGC system in the northern part of the Strait and all along the East Greenland Slope (Figs. 7 and 8). A narrow core of CBDW can be identified against the slope in the EGC at 79.15°N (Fig. 10). The core is centered around 1700 m, the approximate depth below which the thermobaric effect makes the colder, fresher water column of the Greenland Sea denser than the warmer, saltier deep waters of the Arctic Ocean (Aagaard et al 1985). The EBDW is deeper, so that it cannot penetrate freely to the south as the

CBDW outflow. The 2600-m sill prevents most of the EBDW from entering the Greenland Sea. However, a salinity maximum reaching 34.92 and clearly associated with the EBDW is found in the southwestern part of the strait (Fig. 7). Therefore, some EBDW escapes to the south where it finally loses its characteristics when circulating around the Greenland Sea gyres. The salinity maximum associated with the CBDW is still above 34.92 when it exits to the Greenland Sea. The weak salinity maximum ($S \approx 34.92$) found in the southeastern part of the strait, with a temperature of approximately -0.9°C (Fig. 7) may be a remnant of the recirculation of some CBDW around the Greenland Sea gyres. According to Aagaard et al. (1991) the recirculation of the deep saline outflows from the Arctic Ocean results in mixing with fresher products formed through open ocean convection in the gyres. If the salinity maximum in the deep WSC is indeed a signature of the CBDW, it demonstrates a gradual cooling of the core of CBDW on its route through the Arctic Mediterranean. The corresponding maximum in the EGC is warmer by about $0.2 - 0.3^\circ\text{C}$, while the deep water in the Canadian Basin has a temperature higher by another $0.2 - 0.3^\circ\text{C}$ (Fig. 1c).

3.5.3. Nordic Seas deep waters: Greenland Sea Deep Water and Norwegian Sea Deep Water

The coldest water mass in Fram Strait ($\theta < -1.1^\circ\text{C}$), the GSDW, is characterized by a downward salinity decrease to values less than 34.90 (Fig. 3c). This water mass is almost exclusively found south of the sill, in the Boreas Basin (Fig. 7). The GSDW in the Boreas Basin is a slightly modified (more saline and warmer) mode of the pure GSDW formed in the Greenland Basin (Clarke et al. 1990). The GSDW in the Boreas Basin is only slightly denser (when its density is referred to 3000 dbar) than the bottom water on the other side of the sill, that is, the EBDW (Table 1). As it is the densest water mass, the GSDW also fills the deepest layer in the Molloy Deep (Figs. 7 and 10).

The temperature range of the EBDW ($-1.1^\circ\text{C} < \theta < -0.8^\circ\text{C}$) but for a lower salinity ($34.90 < S < 34.92$) defines the cold mode of the NSDW (NSDWc) (Fig. 3). Its characteristics cover the NSDW as defined by Swift & Koltermann (1988) in the Norwegian Sea, i.e. $\theta = -1.05^\circ\text{C}$ and $S = 34.91$. The NSDWc is formed through mixing between the EBDW and the GSDW along the periphery of the Greenland Sea gyres (Smethie et al. 1988, Aagaard et al. 1991). Consequently, the NSDWc is found in Fram Strait in the WSC system (Fig. 7). A possible direct contact between the EBDW and the GSDW over the sill also suggests local formation of NSDWc in Fram Strait.

In Schlichtholz & Houssais (1999b) the warm mode of NSDW (NSDW_w) has been defined as water in the salinity limits of the NSDW_c and covering the temperature range $-0.8^{\circ}\text{C} < \theta < -0.5^{\circ}\text{C}$ but only if the water lies above the NSDW_c, and also the range $-0.5^{\circ}\text{C} < \theta < 0^{\circ}\text{C}$ if the water is not characterized by a clear slope in the $\theta - S$ curve associated with either the AIW or the UPDW (Table 1). Some NSDW_w defined in this way is found, for instance, along the Spitsbergen Slope where the $\theta - S$ curves display little spreading of the salinity values in the deep range (Fig. 7) and the salinity distribution over the slope is rather uniform below 1000 m and within the range of the NSDW (Fig. 9). However, little of NSDW_w is advected to Fram Strait from the south in the WSC system. Much more outflows from the Arctic Ocean in the EGC system. In fact, the NSDW_w in Fram Strait is not a water mass with a well-defined origin but has a rather long mixing history within the Arctic Mediterranean. Some NSDW_w is also formed locally in the strait. The NSDW as a whole has the largest production rate from all the water masses modified in Fram Strait (Schlichtholz & Houssais 1999b).

4. Discussion

A detailed description of the processes determining the water mass transformations in different regions of the Arctic Mediterranean and the connections between the regions has been recently published by Rudels et al. (1999). In Rudels et al. (2000), a water mass analysis was carried out for a particular region, Fram Strait, in which symptoms of all major processes in the Arctic Mediterranean can be tracked through inspection of extremes in the distribution of water mass properties. The present study provides details of the $\theta - S$ structure in the strait based on the largest hydrographic data set ever collected in the area, i.e. the MIZEX 84 stations.

The general picture which emerges from the analysis of the MIZEX 84 data opposes the water masses of the WSC system to the water masses of the EGC system separated by the EGPF (Fig. 5). The front runs approximately from south-west to north-east so that the water masses of the WSC system dominate in the southern part of the strait while the water masses of the EGC system dominate in the northern part. The temperature and salinity contrasts across the front change sign at intermediate depths, with warm and saline water on the WSC side of the front in the upper layer and on the EGC side in the deep layer.

The water masses of the WSC system interact with the water masses of the EGC system as they move northward and southward, respectively. Features related to this interaction are, for instance, the bifurcation of the AW_w in the Yermak Plateau area (the north-eastern boxes in Fig. 6) representing two branches in which the inflow to the Arctic Ocean through

Fram Strait occurs (see also Rudels et al. 2000), or the presence of cores of a relatively warm and saline AW in the southern part of the East Greenland Slope (Fig. 8) indicating local recirculations of the WSC. Results of the interaction between the two systems are also the presence of a warm and fresh mode of AW (AWF) along the ice edge and the abundance of another water mass with no particular signature in the $\theta - S$ space, i.e. the NSDW, in the central part of the strait. Each of these two water masses is partly produced in the strait. Some warm NSDW (NSDW_w) is derived from a transformation of the AIW which is seen as a weakening of the intermediate salinity minimum in the WSC system towards the Arctic Ocean. Only a weak intermediate salinity minimum survives and reaches the Eurasian Basin. Most of the GSDW is topographically constrained to remain south of the Fram Strait sill, but an inflow to the Arctic Ocean of deep water derived from the WSC system can be recognized in a near-bottom salinity decrease present at some stations along the continental slope west of the Yermak Plateau. Very weak signatures of both the AIW and the Nordic Seas deep waters can be tracked around the Yermak Plateau (Rudels et al. 2000).

The intermediate and deep waters of the EGC are modified in Fram Strait but preserve their characteristics better as they pass through the strait than the WSC-derived deep inflow to the Arctic Ocean. (The disappearance of the deep water column typifying the EGC in the south-western box in Fig. 7 and also of the MAW in the corresponding box in Fig. 6 is related to the lack of hydrographic stations over the continental slope in this part of the strait in the MIZEX 84 data set). Although the sill constrains most of the EBDW to remain in the Lena Trough, the warmer part of this water mass passes to the south, where a saline deep outflow from below the level of the CBDW is an essential component of the formation of the NSDW on the periphery of the Greenland gyre (e.g. Aagaard et al. 1991). While some deep water with a CBDW-derived salinity maximum enters the Iceland Sea along the continental slope (e.g. Buch et al. 1996), a core of CBDW recirculates back to Fram Strait, where it appears as a salinity maximum below the AIW in the WSC system. The maximum has $\theta - S$ characteristics of the NSDW as defined in the present study, but would fall within the range of characteristics of the CBDW as defined, for instance, in the classification of water masses in Fram Strait used by Rudels et al. (2000). The deep part of the water column in the rift valley of the Knipovich Ridge resembles the deep part of the water column in the Lena Trough, with a near-bottom, quasi-isothermal salinity jump here being the result rather of haline convection in the north-western Barents Sea, which renews the abyssal waters of the northern Norwegian Sea. The $\theta - S$ characteristics of

the jump remain within the range of the cold mode of the NSDW (NSDWc). However, the saltier part of the jump would be classified as EBDW if the water mass definition of Rudels et al. (2000) was applied. The salinity minimum between the saline near-bottom water and the CBDW-derived salinity maximum is most likely the NSDW from the Norwegian Sea. The presence of a deep water column with water masses of various distinct origins in the Knipovich Ridge area is perhaps the least known aspect of the water mass distribution in Fram Strait. However, the saline near-bottom water in that area may be an intermittent feature (Swift & Koltermann 1988).

The ice and water mass distributions in the Arctic Mediterranean are known to be highly variable on interannual and longer time scales. Some of this variability has been attributed to variations in the exchanges through Fram Strait. The Great Salinity Anomaly propagating around the northern North Atlantic from the late 1960s to the early 1980s (Dickson et al. 1988) is thought to have been related to anomalous ice and fresh water export through Fram Strait (e.g. Aagaard & Carmack 1989), while the warming of the AW layer in the Arctic Ocean in the 1990s (Carmack et al. 1995, Grotedefdt et al. 1998, Zhang et al. 1998) could be linked to variations in the magnitude and characteristics of the AW inflow through Fram Strait and over the Barents Sea. Such variations are closely related to the North Atlantic Oscillation (e.g. Dickson et al. 2000), as may also be the composition of the deep water masses (e.g. Dickson et al. 1996). More recently, Rudels et al. (2000) suggested that changes in the exchanges through Fram Strait could also be related to the change in the renewal of dense waters in the Greenland Sea, which reached deep layers in the 1980s and only intermediate layers in the 1990s (Budéus et al. 1998). By comparing the summer $\theta - S$ structure at 79°N in 1997 with the corresponding structure in 1984, using for the latter a subset of the data analyzed in the present study, they found cooler, fresher and denser deep layers as well as a larger westward extension of the recirculating AW in 1984 as compared with 1997. Rudels et al. concluded that such modifications could be responsible for concomitant modifications of the circulation in Fram Strait. A more intense AW exchange between the Nordic Seas and the Arctic Ocean (as in 1997) could alternate with a stronger recirculation of the WSC (as in 1984). Larger exchanges through Fram Strait in the 1990s than in the 1980s seem to be confirmed by transport estimates. The estimates of the mean northward and southward transports at 79°N of 6.9 Sv and 11.1 Sv respectively from the late 1990s (Fahrback et al. 2000) are much larger than the estimates from the early 1980s (Rudels 1987, Schlichtholz & Houssais 1999a). However, part of the discrepancy is most probably due to the seasonality of the flow reported, for instance, in the same study by

Fahrbach et al. (2000). Part may be also methodological: while the estimates of Rudels (1987) and Schlichtholz & Houssais (1999a) were based on inverse modeling, the estimates of Fahrbach et al. (2000) were obtained from direct current measurements along a section of moorings.

The influence of Fram Strait on climatic variability goes well beyond the Arctic Mediterranean. The main part of the surface PW in the EGC flows out through the Denmark Strait, while the maximum temperature layer contributes, through mixing with the AIW from the Greenland Sea, to the formation of the Denmark Strait Overflow Water (Strass et al. 1993). Rudels et al. (1999) even suggested that the EGC water masses are also important for the outflow through the Faeroe-Shetland Channel.

Acknowledgements

The authors acknowledge the anonymous reviewer for his/her helpful comments.

References

- Aagaard K., Carmack E. C., 1989, *The role of sea ice and other fresh water in the Arctic circulation*, J. Geophys. Res., 94, 14,485–14,498.
- Aagaard K., Fahrbach E., Meincke J., Swift J. H., 1991, *Saline outflow from the Arctic Ocean: Its contribution to the deep waters of the Greenland, Norwegian, and Iceland Seas*, J. Geophys. Res., 96, 4833–4846.
- Aagaard K., Greisman L. K., 1975, *Toward new mass and heat budgets for the Arctic*, J. Geophys. Res., 80, 3821–3827.
- Aagaard K., Swift J. H., Carmack E. C., 1985, *Thermohaline circulation in the Arctic Mediterranean Seas*, J. Geophys. Res., 90, 4833–4846.
- Anderson L. G., Björk G., Holby O., Jones E., Kattner P. K., Lilieblad B., Rudels B., Swift J. H., 1994, *Water masses and circulation in the Eurasian Basin: Results from the Oden 91 expedition*, J. Geophys. Res., 99, 3273–3283.
- Anderson L. G., Jones E. P., Koltermann K. P., Schlosser P., Swift J. H., Wallace D. W. R., 1989, *The first oceanographic section across the Nansen Basin in the Arctic Ocean*, Deep-Sea Res., 36, 475–482.
- Bourke R. H., Newton J. L., Paquette R. G., Tunnicliffe M. D., 1987, *Circulation and water masses of the East Greenland Shelf*, J. Geophys. Res., 92, 6729–6740.
- Boyd T. J., D'Asaro E. A., 1994, *Cooling of the West Spitsbergen Current*, J. Geophys. Res., 99, 22,597–22,618.
- Buch E., Malmberg S.-A., Kristmannsson S. S., 1996, *Arctic Ocean deep water masses in the western Iceland Sea*, J. Geophys. Res., 101, 11965–11973.

- Budéus G., Schneider W., Krause G., 1998, *Winter convective events and bottom water warming in the Greenland Sea*, J. Geophys. Res., 103, 18,513–18,528.
- Carmack E. C., Macdonald R. W., Perkin R. G., McLaughlin A., 1995, *Evidence for warming of Atlantic water in the southern Canadian Basin of the Arctic Ocean: Results from the Larsen-93 expedition*, Geophys. Res. Lett., 22, 1061–1064.
- Clarke R. A., Swift J. H., Reid J. L., Koltermann K. P., 1990, *The formation of Greenland Sea Deep Water: Double diffusion or deep convection?*, Deep-Sea Res., 37, 1385–1424.
- Dickson R., Lazier J., Meincke J., Rhines P., Swift J. H., 1996, *Long-term coordinated changes in the convective activity of the North Atlantic*, Prog. Oceanogr., 38, 241–295.
- Dickson R. R., Meincke J., Malmberg S. A., Lee A. J., 1988, *The ‘Great Salinity Anomaly’ in the northern North Atlantic*, Prog. Oceanogr., 20, 103–151.
- Dickson R. R., Osborn T. J., Hurrell J. W., Meincke J., Blindheim J., Adlandsvik B., Vinje T., Alekseev G., Maslowski W., 2000, *The Arctic Ocean response to the North Atlantic Oscillation*, J. Climate, 13, 2671–2696.
- Fahrbach E., Meincke J., Østerhus S., Rohardt G., Schauer U., Tverberg V., Verduin J., 2000, *Direct measurements of volume transports through Fram Strait*, Polar Res., 20, 217–224.
- Friedrich H., Houssais M.-N., Quadfasel D., Rudels B., 1995, *On Fram Strait water masses*, Nordic Seas Symp., Extended abstract, Hamburg 7 March–9 March, 69–72.
- Gascard J.-C., Kergomard C., Jeannin P.-F., Fily M., 1988, *Diagnostic study of the Fram Strait marginal ice zone during summer from 1983 and 1984 Marginal Ice Zone Experiment lagrangian observations*, J. Geophys. Res., 93, 3613–3641.
- Grotefendt K., Logemann K., Quadfasel D., Ronski D., 1998, *Is the Arctic Ocean warming?*, J. Geophys. Res., 103, 27,679–27,687.
- Hunkins K., 1990, *A review of the physical oceanography of Fram Strait*, [in:] *The physical oceanography of Sea Straits*, I. Pratt (ed.), Kluwer Acad. Publ., Netherlands, 61–93.
- Johannessen J. A., Johannessen O. M., Svendsen E., Shuchman R., Manley T., Campbell W. J., Josberger E. G., Sandven S., Gascard J.-C., Olaussen T., Davidson K., Van Leer J., 1987, *Mesoscale eddies in Fram Strait marginal ice zone during the 1983 and 1984 Marginal Ice Zone Experiments*, J. Geophys. Res., 92, 6754–6772.
- Jones E. P., Rudels B., Anderson L. G., 1995, *Deep waters of the Arctic Ocean: origins and circulation*, Deep-Sea Res., 42, 737–760.
- Josberger E. G., 1987, *Bottom ablation and heat transfer coefficients from the 1983 Marginal Ice Zone experiments*, J. Geophys. Res., 92, 7012–7016.
- Morison J. H., McPhee M. G., Maykut G. A., 1987, *Boundary layer, upper ocean, and ice observations in the Greenland Sea marginal ice zone*, J. Geophys. Res., 92, 6987–7011.

- Muench R.D., McPhee M.G., Paulson C.A., Morison J., 1992, *Winter oceanographic conditions in the Fram Strait-Yermak Plateau region*, J. Geophys. Res., 97, 3469–3484.
- Quadfasel D., Rudels B., Kurtz K., 1988, *Outflow of dense water from a Svalbard fjord into the Fram Strait*, Deep-Sea Res., 35, 1143–1150.
- Rudels B., 1987, *On the mass balance of the Polar Ocean with special emphasis on the Fram Strait*, Norsk Polarinst. Skr., 188, 1–53.
- Rudels B., 1989, *The formation of polar surface water, the ice export and the exchanges through the Fram Strait*, Prog. Oceanogr., 22, 205–248.
- Rudels B., Friedrich H. J., Quadfasel D., 1999, *The Arctic Circumpolar Boundary Current*, Deep-Sea Res., Part II, 46, 1023–1062.
- Rudels B., Jones E.P., Anderson L.G., Kattner G., 1994, *On the intermediate depth waters of the Arctic Ocean*, [in:] *The role of the Polar Oceans in shaping the global climate*, R. Muench, O. Johannessen (eds.), Amer. Geophys. Union, New York, 33–46.
- Rudels B., Meyer R., Fahrbach E., Ivanov V. V., Østerhus S., Quadfasel D., 2000, *Water mass distribution in Fram Strait and over the Yermak Plateau*, Ann. Geophys., 18, 687–705.
- Rudels B., Quadfasel D., 1991, *Convection and deep water formation in the Arctic Ocean – Greenland Sea System*, J. Mar. Sys., 2, 435–450.
- Schauer U., 1995, *The release of brine-enriched shelf water from Storfjord into the Norwegian Sea*, J. Geophys. Res., 100, 16,015–16,028.
- Schauer U., Muench R. D., Rudels B., Timokhov L., 1997, *Impact of eastern Arctic shelf waters on the Nansen Basin intermediate layers*, J. Geophys. Res., 102, 3371–3382.
- Schlichtholz P., Houssais M.-N., 1999a, *An inverse modeling study in Fram Strait. Part I: Dynamics and circulation*, Deep-Sea Res., Part II, 46, 1083–1135.
- Schlichtholz P., Houssais M.-N., 1999b, *An inverse modeling study in Fram Strait. Part II: Water mass distribution and transports*, Deep-Sea Res., Part II, 46, 1137–1168.
- Schlichtholz P., Houssais M.-N., 1999c, *An investigation of the dynamics of the East Greenland Current in Fram Strait based on a simple analytical model*, J. Phys. Oceanogr., 29, 2240–2265.
- Smethie W.M., Chipman J.D.W., Swift J.H., Koltermann K.P., 1988, *Chlorofluoromethanes in the Arctic Mediterranean seas: evidence for formation of bottom water in the Eurasian Basin and deep water exchange through Fram Strait*, Deep-Sea Res., 35, 347–369.
- Strass V., Fahrbach E., Schauer U., Sellmann L., 1993, *Formation of Denmark Strait overflow water by mixing in the East Greenland Current*, J. Geophys. Res., 98, 6907–6919.
- Swift J.H., 1986, *The Arctic Waters*, [in:] *The Nordic Seas*, B.G. Hurdle (ed.), Springer-Verlag, New York–Berlin, 129–153.

- Swift J.H., Aagaard K., 1981, *Seasonal transitions and water mass formation in the Iceland and Greenland Seas*, Deep-Sea Res., 28A, 1107–1129.
- Swift J.H., Koltermann K.P., 1988, *The origin of Norwegian Sea Deep Water*, J. Geophys. Res, 93, 3563–3569.
- Zhang J.D., Rothrock D.A., Steele M., 1998, *Warming of the Arctic Ocean by a strengthened Atlantic inflow: Model results*, Geophys. Res. Lett., 25, 1745–1748.